Dual-PEEC Modeling of a Two-Port TEM Cell for VHF Applications

P. Alotto[(1)], D. Desideri[(1)], F. Freschi[(2)], A. Maschio[(1)], M. Repetto[(2)]
[(1)] Università degli Studi di Padova, Dept of Electrical Engineering, Padova, Italy
[(2)] Politecnico di Torino, Dept of Electrical Engineering, Torino, Italy

Two-port TEM cells with rectangular cross-section are commonly used to produce plane electromagnetic waves with high electric field. The non-uniform structure makes the use of numerical methods extremely useful in the design phase in order to achieve a very good behavior of the TEM cell over a wide frequency range of operation. In this paper an extended version of PEEC is used to study a real device and results are compared with experimental ones.

***Index Terms*—partial element equivalent circuit, tem cell**

I. Introduction

TEM cells provide a low-cost solution for the generation of high-frequency fields in small space volumes and are thus very well suited for many applications like probe calibration, biomedical studies and EMC tests. Although design rules for such systems can be traced back to the original work of Crawford [1] the performance of such systems over wide frequency ranges depends critically on the design of the terminations and of the tapered transitions and numerical modeling significantly reduces the need for prototypes. In this paper an improved PEEC formulation which allows the use of the triangular elements needed for accurately modeling the terminations is presented and results are compared with experimental ones.

II. Dual-PEEC formulation

The Partial Element Equivalent Circuit (PEEC), is a well assessed integral technique whose origins go back to the middle '70s in the seminal work by Ruehli [2]. The basic idea is simulate an electromagnetic structure by means of an equivalent lumped circuit which can then be solved by SPICE-like circuit simulators. The starting point is the equation of the total electric field which, at the observation point $\vec{r}$ and angular frequency ω, takes the form:

$$\frac{\vec{J}(\vec{r},\omega)}{\sigma} = -\mathrm{j}\omega\vec{A}(\vec{r},\omega) - \nabla\varphi(\vec{r},\omega). \tag{1}$$

where $\vec{J}$ is the current density, $\vec{A}$ and φ are the retarded magnetic vector and electric scalar potential, respectively, which can be expressed as:

$$\vec{A}(\vec{r},\omega) = \frac{\mu}{4\pi}\int_\Omega \frac{\vec{J}(\vec{r}',\omega)}{|\vec{r}-\vec{r}'|}\mathrm{e}^{-\mathrm{j}\beta|\vec{r}-\vec{r}'|}\mathrm{d}\Omega \tag{2}$$

$$\varphi(\vec{r},\omega) = \frac{1}{4\pi\epsilon}\int_\Omega \frac{\rho(\vec{r}',\omega)}{|\vec{r}-\vec{r}'|}\mathrm{e}^{-\mathrm{j}\beta|\vec{r}-\vec{r}'|}\mathrm{d}\Omega \tag{3}$$

Manuscript received May 31, 2010. Corresponding author: P. Alotto (e-mail: alotto@die.unipd.it).

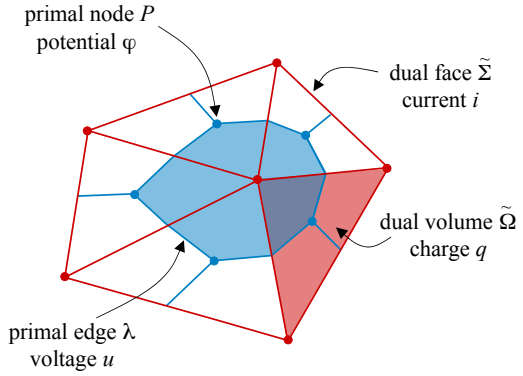

Fig. 1. Surface discretization: primal and dual complex.

TABLE I
Variable assignment to spatial elements

Variable	Spatial Element	Geometry
current, i	dual face, $\tilde{\Sigma}$	triangle side × depth
charge, q	dual volume, $\tilde{\Omega}$	triangle × depth
voltage, u	primal edge, λ	piecewise segment
potential, φ	primal node P	centroid of triangle

where ρ is the volume charge density, β is the wavenumber, $\vec{r}'$ the source point and Ω the conductor domain. By substituting (2) and (3) in (1) the well-known EFIE equation is obtained:

$$\begin{aligned}\frac{\vec{J}(\vec{r},\omega)}{\sigma} = &-\frac{\mathrm{j}\omega\mu}{4\pi}\int_\Omega \frac{\vec{J}(\vec{r}',\omega)}{|\vec{r}-\vec{r}'|}\mathrm{e}^{-\mathrm{j}\beta|\vec{r}-\vec{r}'|}\mathrm{d}\Omega \\ &-\frac{1}{4\pi\epsilon}\nabla\int_\Omega \frac{\rho(\vec{r}',\omega)}{|\vec{r}-\vec{r}'|}\mathrm{e}^{-\mathrm{j}\beta|\vec{r}-\vec{r}'|}\mathrm{d}\Omega.\end{aligned} \tag{4}$$

Differently from the standard PEEC formulation (e.g. [3] [4]) equation (4) is discretized by using two grids of interlocked cells, called primal and dual discretization. Variables are associated to different spatial elements, according to the work of Tonti [5], and as shown in Table I and Fig. 1. The resulting discretization method is called dual-PEEC [6]. This

new framework for the PEEC method allows the use of general meshes consisting of a mixture of triangles and quadrilaterals, as detailed in [7]. In this paper we restrict the formulation to triangular surface elements only.

In each triangle m, and defining t_m the thickness of the conductor, the current density is expanded by means of div-conforming [8] facet basis functions $\vec{w}_{km}$:

$$\vec{J}_m = \frac{1}{t_m} \sum_{k=1}^{3} \vec{w}_{km} i_{km} \tag{5}$$

where i_{km} is the electric current flowing through the kth edge of triangle m. The surface charge density δ_m is considered uniform in the mth element, so that:

$$\delta_m = \frac{q_m}{S_m} \tag{6}$$

where q_m and S_m are the total charge and the area of triangle m. The coefficient $1/S_m$ can be considered as the constant basis function used to expand the charge density δ_m, respectively.

By substituting (5) and (6) into (4) discretized over a triangular mesh, and restricting the integration domain over surface elements

$$\sum_m \frac{\sum_{k=1}^{3} \vec{w}_{km} i_{km}}{t_m \sigma} = -\frac{\mathrm{j}\omega\mu}{4\pi} \sum_m \int_{\Sigma_m} \frac{\sum_{k=1}^{3} \vec{w}_{km}(\vec{r}') i_{km}(\omega)}{|\vec{r} - \vec{r}'|} \mathrm{e}^{-\mathrm{j}\beta|\vec{r}-\vec{r}'|} \mathrm{d}\Sigma \tag{7}$$
$$-\frac{1}{4\pi\epsilon} \sum_m \nabla \int_{\Sigma_m} \frac{q_m(\omega)}{S_m |\vec{r} - \vec{r}'|} \mathrm{e}^{-\mathrm{j}\beta|\vec{r}-\vec{r}'|} \mathrm{d}\Sigma.$$

Basis functions (5) and (6) are also used as test functions of (7), resulting in a Galerkin scheme. After this step each term of (7) can be interpreted as a discrete circuit element (*partial element*):

- partial resistances, which take into account the ohmic losses in the conductor, neglected in this study;
- partial inductances, which model the inductive coupling between the kth current of element m and the hth current of element n:

$$L_{km,hn} = \frac{\mu_0}{4\pi} \int_{\Sigma_m} \vec{w}_{km} \cdot \int_{\Sigma_n} \frac{\vec{w}_{hn}}{|\vec{r} - \vec{r}'|} \mathrm{d}\Sigma_n \mathrm{d}\Sigma_m; \tag{8}$$

- partial potential coefficients, which measure the contribution of the charge in cell n to the voltage of cell m:

$$p_{m,n} = \frac{1}{4\pi\epsilon_0 S_m S_n} \int_{\Sigma_m} \int_{\Sigma_n} \frac{1}{|\vec{r} - \vec{r}'|} \mathrm{d}\Sigma_n \mathrm{d}\Sigma_m. \tag{9}$$

The corresponding retarded coefficients can be derived by introducing the retarded coefficients: $L_{km,hn}\mathrm{e}^{-\mathrm{j}\beta|\vec{r}_{km}-\vec{r}_{hn}|}$, $p_{m,n}\mathrm{e}^{-\mathrm{j}\beta|\vec{r}_m-\vec{r}_n|}$. The reader may refer to [7] for a detailed description of the partial elements and for an alternative derivation of their definition. The equivalent two-terminal component is shown in Fig. 2. The dual-PEEC two terminal components can be assembled to obtain the complete circuit to be solved by a general purpose SPICE-like network simulator.

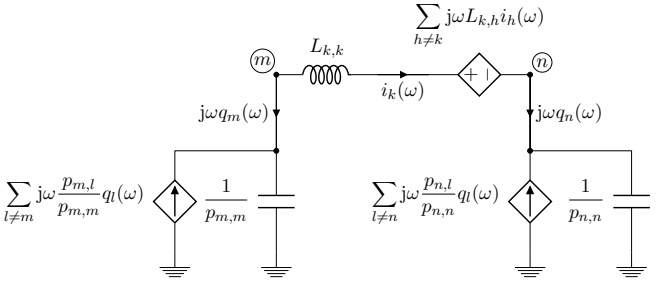

Fig. 2. PEEC equivalent circuit.

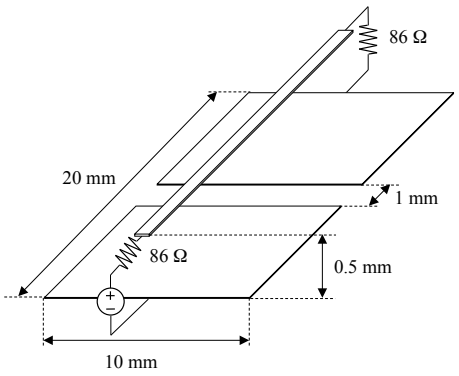

Fig. 3. Benchmark problem used in the accuracy assessment of dual-PEEC.

III. Accuracy assessment

The geometry of the TEM cell under study includes parts with a very small thickness, in particular the central septum. On the other side, the thickness has non-negligible effects on the operation of the cell and thus a thin shell model is not appropriate for the simulation. The discretization of such an object, requires a surface mesh made of triangles, where elements on the thickness have very large aspect ratios. From the literature it is not clear how the shape of elements will affect the accuracy of solution, and for this reason a preliminary study on the accuracy of solutions with low-quality elements is required. To this purpose the microstrip over a split ground plane of Fig. 3 is studied. Results relative to the input impedance in the range $1-10$ GHz are available in the literature [9] and obtained by the standard PEEC method. The structure is modeled by assigning to each electrode a finite thickness of 10^{-4} mm, while triangles on the surface have edges with average length of 1.4 mm. This ensures a sufficient number of elements per wavelength. The elements in the thickness have four order of magnitude between the largest and the shortest edge. As it can be seen in Fig. 4, the dual-PEEC solution maintains a good accuracy also with poorly shaped elements, and is thus suitable for characterizing the behavior of the TEM cell.

IV. TEM cell description and operation

A. TEM cell description

The previous numerical model has been applied to a two-port TEM cell, designed and realized at the Department of Electrical Engineering of the University of Padova [10]. In

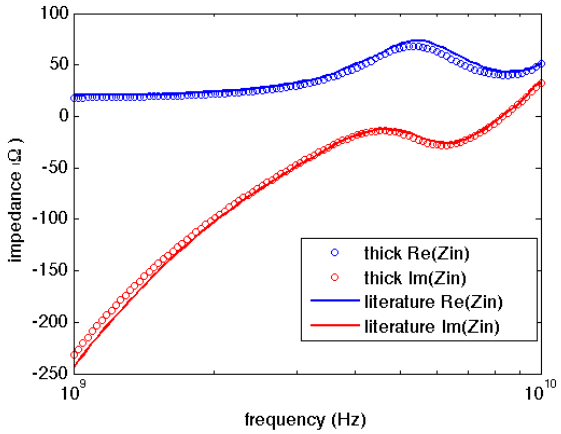

Fig. 4. Accuracy assessment for highly distorted elements.

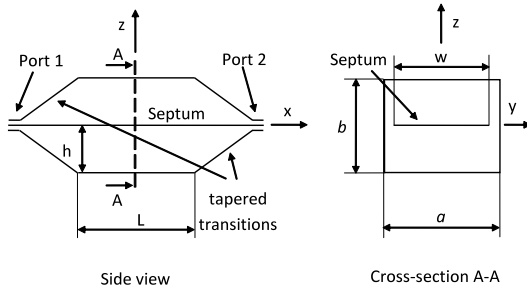

Fig. 5. Side view and cross-section of the two-port TEM cell outline, with reference axis.

Fig. 5 a schematic view of the TEM cell is presented. This device has a rectangular cross-section of the central part, with $a = 450$ mm and $b = 360$ mm. The outer conductor is in aluminum; the inner conductor (septum) is in brass, 1.5 mm thick. A plane view of the septum is reported in Fig. 6. It can be seen that there are two critical parts: one corresponds to the tapered transitions, that join the central rectangular part to a smaller straight rectangular part near each termination; the second one is the final transition to each end connector, that has been here realized with a triangular shape, as outlined in black in Fig. 6. For ease of welding, this final triangular transitions have been done in copper, and are 0.6 mm thick.

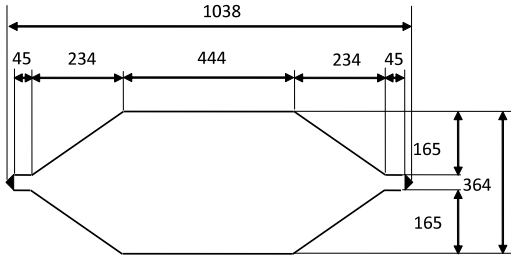

Fig. 6. Septum plane view.

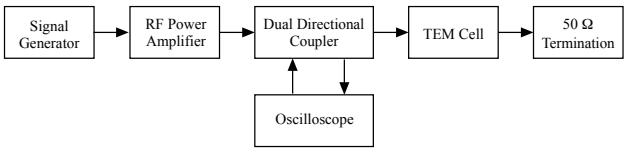

(a)

(b)

Fig. 7. TEM cell: (a) block diagram of the measurement system, and (b) experimental setup.

B. TEM cell operation

The TEM cell has been designed for a highest test frequency of 230 MHz. Its standard use is in combination with a test system (frequency range 10 kHz – 230 MHz), which can be seen in Fig. 7. It is composed by: a signal generator with a power RF amplifier (35 W nominal output CW power, 10 kHz–250 MHz frequency response), connected to the TEM cell through a dual directional coupler (10 kHz – 400 MHz frequency range) and a 50 Ω matched termination (nominal TEM cell characteristic impedance is 50 Ω).

The dual directional coupler allows to obtain two voltage signals proportional to the forward– and backward–traveling waves respectively. These signals have been acquired by a 1 GHz bandwidth oscilloscope and used for the Voltage Standing Wave Ratio (VSWR) calculation which is a commonly used quality indicator for the performance of TEM cells [10], [11].

V. Numerical Results

The numerical results presented in this section are related to the analysis of the VSWR which for a matched termination is defined by:

$$\mathrm{VSWR} = \frac{1 + |S_{11}|}{1 - |S_{11}|} \tag{10}$$

where the scattering parameter $|S_{11}|$ is easily computed from the port impedance matrix provided by the dual-PEEC method. Fig. 8 shows the mesh used to model one of the terminations and clearly demonstrates the usefulness of triangular meshes for this class of applications.

Fig. 9 shows the comparison between experimental results and computed results with various mesh sizes. A mesh consisting of roughly 5500 triangular elements is sufficient to get converged results and further refinement does not alter them

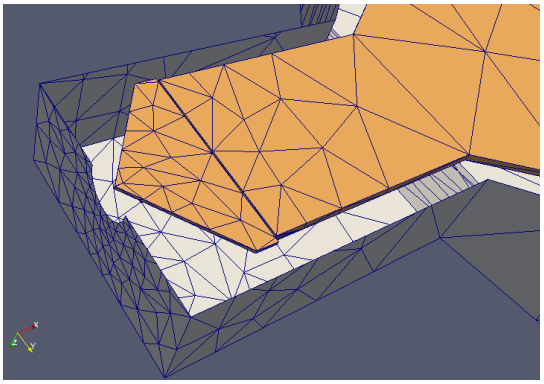

Fig. 8. Detail of the mesh in the neighborhood of a termination.

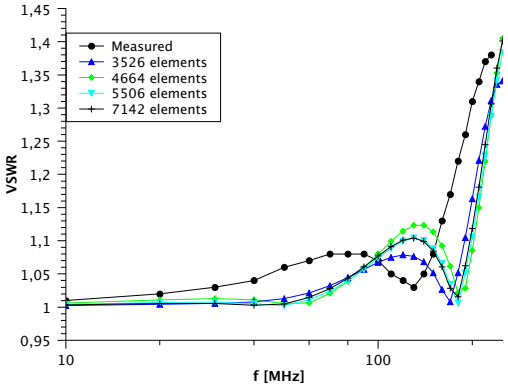

Fig. 9. Experimental and computed results with various mesh sizes.

significantly. The implemented code running on a 2 quad-core Intel Xeon E5440 2.83 GHz with 32 GB RAM takes 860 s for the computation of the coefficients and 67 s for the solution at each frequency for a total runtime of 2540 s. The code is implemented in the Matlab environment with some performance critical routines written in Fortran 90 and evaluates the coefficients in parallel. Furthermore, also the solver is parallelized through the use of the parallel Lapack features of Matlab and profiling shows that all cores run at full speed during the solution phase.

A. Critical analysis

The previous results show a generally satisfactory agreement between measured and computed results. Anyway, some efforts have been devoted to a further investigation of the obtained numerical data. Indeed simulation results refer to the cell as designed and not as actually manufactured. Possible causes of error include angular deviations especially in the tapered transitions, misalignment and non-planarity of the septum, lack of some features in the model (e.g. dielectric support pillars). Simulations show a very small sensitivity of the VSWR with respect to small lateral misalignments of the septum (2 mm), as shown in Fig. 10 for the case of 5506 elements, whereas vertical movements reduce the height of the 150 MHz peak, which may indicate that the septum is not exactly in the vertical middle of the constructed TEM

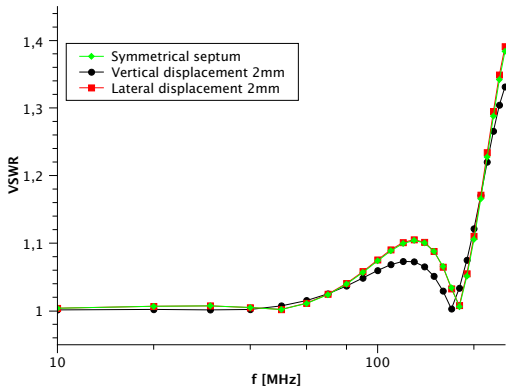

Fig. 10. Effect of vertical and lateral displacement of the septum.

cell. Currently our PEEC formulation is being extended in order to allow the inclusion of dielectric volumes which could further improve the correspondence between simulations and experiments.

VI. Conclusions

In this paper an improved PEEC formulation which allows the use of triangular elements has been applied to the study of a TEM cell for VHF applications. Computational results are in good agreement with experimental ones and indicate the usefulness of triangular elements in modeling the septum terminations. Further investigations are underway in order to asses the sensitivity of the model to manufacturing tolerances and to the presence of the dielectric pillars sustaining the septum.

References

[1] M. Crawford, "Generation of standard EM fields using TEM transmission cells," *IEEE Transactions on Electromagnetic Compatibility*, vol. 16, no. 4, pp. 189–195, 1974.

[2] A. Ruehli, "Equivalent circuit models for three-dimensional multiconductor systems," *IEEE Transactions on Microwave Theory and Techniques*, vol. 22, pp. 216–221, 1974.

[3] H. Heeb and A. Ruehli, "Three-dimensional interconnect analysis using partial element equivalent circuits," *IEEE Transactions on Circuits and Systems I: Fundamental Theory and Applications*, vol. 39, no. 11, pp. 974–982, Nov 1992.

[4] J. Garrett, "Advancements of the partial element equivalent circuit formulation," Ph.D. dissertation, University of Kentucky, 1997.

[5] E. Tonti, "Finite Formulation of Electromagnetic Field," *IEEE Transactions on Magnetics*, vol. 38, pp. 333–336, 2002.

[6] F. Freschi, G. Gruosso, and M. Repetto, "Unstructured PEEC Formulation by Dual Discretization," *IEEE Microwave and Wireless Components Letters*, vol. 16, no. 10, pp. 531–533, Oct 2006.

[7] F. Freschi and M. Repetto, "A general framework for mixed structured/unstructured peec modelling," *ACES Journal*, vol. 23, no. 3, pp. 200–206, Sep 2008.

[8] S. Rao, D. Wilton, and A. Glisson, "Electromagnetic scattering by surface of arbitrary shape," *IEEE Transactions on Antennas and Propagation*, vol. 30, pp. 409—418, 1982.

[9] W. Pinello, A. Ruehli, and A. Cangellaris, "Analysis of interconnect and package structures using PEEC models with radiated emissions," *IEEE International Symposium on Electromagnetic Compatibility*, pp. 353 – 358, 1997.

[10] D. Desideri and A. Maschio, "Preliminary tests on a low cost two-port TEM cell," *Acta Electrotehnica – Special Issue 2008*, pp. 298–301, 2008.

[11] IEC Standard 62132-2: 2010-03, "Integrated circuits - Measurement of electromagnetic immunity. Part 2: Measurement of radiated immunity - TEM cell and wideband TEM cell method," 2010.